SENSOR LETTERS
Vol. 7, 1–6, 2009

Electromagnetic Field Computation in Magnetic and Conductive Thin Sheets

Alejandro Ospina*, Laurent Santandrea, Yann Le Bihan, and Claude Marchand

Laboratoire de Génie Electrique de Paris, CNRS UMR8507; SUPELEC; UPMC Univ Paris 06; Univ Paris-Sud; 11 rue Joliot-Curie, Plateau de Moulon, 91192 Gif-sur-Yvette Cedex, France

(Received: 29 February 2008. Accepted: 23 February 2009)

The finite element method (FEM) is one of the most important techniques of computer modeling because it has a high geometric adaptation capability that makes possible the computation of a great variety of configurations. Nevertheless, the study of special structures that have a geometric dimension smaller than others, creates meshing difficulties. In this paper, the use of shell elements for modeling magnetic and/or conductive thin regions in finite element method is presented. This approach avoids the meshing problems of thin regions. The weak formulation is based on $\boldsymbol{a}^*$ for (2D) problem and $\boldsymbol{t}$-ϕ for (3D) problem. The results are compared with analytic exact solutions.

Keywords: Finite Element Method, Shell Elements, Eddy Current Sensors, Thin Regions.

RESEARCH ARTICLE

1. INTRODUCTION

The finite element method (FEM) is one of the most important techniques of computer modeling because it has a high geometric adaptation capability that makes possible the computation of a great variety of configurations. However, the study of special structures that have a geometric dimension smaller than others, creates meshing difficulties (i.e., high element densities, deformed elements). A great number of these thin structures (e.g., thin cracks, coatings, deposits, flat coils…) are encountered in eddy current (EC) testing and in magnetic sensors.

Abundant researches are developed concerning the numerical modeling of thin regions. Among them, three are most usually used. The first is based on the boundary integral, method[1,2] the second combines the finite element resolution with boundary conditions in the low thickness zone.[3,4] In the last, a kind of degenerated finite elements (shell elements) is used to represent the thin regions.[5] These approaches avoids the problems related to the meshing of thin regions. In particular, the last provide a more general description of the physical phenomena that don't take any particular hypothese about the fields inside the thin region. These elements are built converting a volume element into a two-dimensional one or a surface element in a one dimensional element. The aim of this work is to illustrate the use of these special elements in an ECT problem resolution, that will be implemented with two well known electromagnetic formulations: the electric formulation (with the modified magnetic vector potential $\boldsymbol{a}^*$) and the magnetic formulation (with the electric vector and the magnetic scalar potentials $\boldsymbol{t}-\phi$). These two formulations have a rapid convergence and exhibits interesting complementary solutions. The accuracy of problem modeling is established with analytical equations of a classical EC testing problem.

2. PROBLEM DESCRIPTION

The basic geometric configuration is a classical problem in EC: a coil placed above a metallic or ferromagnetic material (Fig. 1), this geometry has an axisymmetrical property that will be used by the formulations. The problem domain Ω is decomposed in three regions: the target material (conducting and/or ferromagnetic) Ω_c, the coil domain Ω_0 and the air region. In our example, the thin region is the conducting and/or ferromagnetic material. The coil has a current density $\boldsymbol{j}_0$ and the thickness of the thin region is denoted by d.

The physical problem in Ω is described by the Maxwell's equations

$$\begin{aligned} &\boldsymbol{curl}(\boldsymbol{h}) = \boldsymbol{j}_0 + \boldsymbol{j}; \qquad \boldsymbol{curl}(\boldsymbol{e}) = -\partial_t\, \boldsymbol{b} \\ &div(\boldsymbol{b}) = 0; \qquad \boldsymbol{b} = \mu \boldsymbol{h}; \qquad \boldsymbol{j} = \sigma \boldsymbol{e} \end{aligned} \tag{1}$$

*Corresponding author; E-mail: alejandro.ospina@lgep.supelec.fr

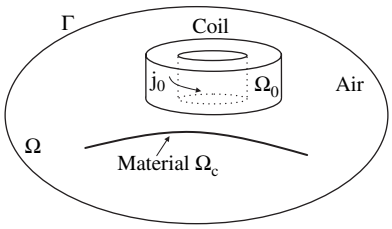

Fig. 1. Problem description.

where $\boldsymbol{h}$ is the magnetic field, $\boldsymbol{b}$ is the magnetic flux density, $\boldsymbol{e}$ is the electric field and $\boldsymbol{j}$ is the current density. The displacement currents are neglected.

3. MAGNETODYNAMIC FORMULATIONS

Two classical formulations for EC problems are proposed to illustrate the computation of the fields in the region Ω because of their interesting complementary properties and the fast algebraic system inversion process. In the electric formulation, the electric field $\boldsymbol{e}$ is associated with a modified magnetic vector potential $\boldsymbol{a}^*$. In the magnetic formulation, the magnetic field $\boldsymbol{h}$ is decomposed in two potentials $\boldsymbol{t}$ and ϕ.

3.1. The Electric Formulation a^*

The electric field is associated with a modified magnetic vector potential so that $\boldsymbol{a}^* = -\int_0^t \boldsymbol{e}\, dt$. In this way, the Ampere's law becomes for $t > 0$ and in the harmonic state:

$$\boldsymbol{curl}\left(\frac{1}{\mu}\boldsymbol{curl}\,\boldsymbol{a}^*\right) = \boldsymbol{j}_0 - i\omega\sigma\boldsymbol{a}^* \tag{2}$$

The weak form of Eq. (2) becomes

$$\begin{aligned}\int_\Omega \frac{1}{\mu}\boldsymbol{curl}\,\boldsymbol{a}^* \cdot \boldsymbol{curl}\,\boldsymbol{a}'\, d\Omega + \int_\Gamma (\boldsymbol{n}\times\boldsymbol{h}^*)\cdot\boldsymbol{a}'\, d\Gamma \\ = \int_\Omega \boldsymbol{j}_0\cdot\boldsymbol{a}'\, d\Omega - \int_\Omega i\omega\sigma\boldsymbol{a}^*\cdot\boldsymbol{a}'\, d\Omega\end{aligned} \tag{3}$$

3.2. The Magnetic Formulation $t-\phi$

In this formulation, the magnetic field is decomposed in an electric vector potential $\boldsymbol{t}$ and in a magnetic scalar potential ϕ so that $\boldsymbol{h} = \boldsymbol{t} - \boldsymbol{grad}\ \phi$. The Faraday's law becomes:

$$\boldsymbol{curl}\left(\frac{1}{\sigma}\boldsymbol{curl}\,\boldsymbol{t}\right) = -i\omega\mu(\boldsymbol{t} - \boldsymbol{grad}\,\phi) \tag{4}$$

The weak form of Eq. (4) is:

$$\begin{aligned}\int_{\Omega_c} \frac{1}{\sigma}\boldsymbol{curl}\,\boldsymbol{t}\cdot\boldsymbol{curl}\,\boldsymbol{t}'\, d\Omega + \int_{\Gamma_c}(\boldsymbol{n}\times\boldsymbol{e})\cdot\boldsymbol{t}'\, d\Gamma \\ = \int_{\Omega_c} i\omega\mu\ \boldsymbol{t}\cdot\boldsymbol{t}'\ d\Omega - \int_{\Omega_c} i\omega\mu\ \boldsymbol{grad}\,\phi\cdot\boldsymbol{t}'\, d\Omega\end{aligned} \tag{5}$$

this last equation is only valid in conductive media, it is necessary for computing the field in all regions to use other property, the $div\,\boldsymbol{b} = 0$ will be verified. This equation is multiplied by $i\omega$ in order to establish the same terms that in Eq. (5). This condition expressed in function of potentials becomes:

$$div(i\omega\boldsymbol{b}) = div(i\omega\mu(\boldsymbol{t} + \boldsymbol{t}_0 - \boldsymbol{grad}\,\phi)) \tag{6}$$

where $\boldsymbol{t}_0$ represents the current sources ($\boldsymbol{j}_0 = \boldsymbol{curl}\,\boldsymbol{t}_0$). The weak form is expressed as:

$$\begin{aligned}\int_\Omega i\omega\mu\ \boldsymbol{grad}\,\phi\cdot\boldsymbol{grad}\,\phi'\, d\Omega + \int_\Gamma i\omega(\boldsymbol{n}\cdot\boldsymbol{b})\phi'\, d\Gamma \\ - \int_\Omega i\omega\mu\ \boldsymbol{t}\cdot\boldsymbol{grad}\,\phi'\, d\Omega \\ - \int_\Omega i\omega\mu\ \boldsymbol{t}_0\cdot\boldsymbol{grad}\,\phi'\ d\Omega = 0\ .\end{aligned} \tag{7}$$

4. THE SHELL ELEMENTS

The degenerated Whitney elements are introduced to avoid the meshing problems in thin regions. These regions are replaced by a D-1 geometric objects (where D is the geometric dimension of the problem): the removed dimension which corresponds to the thickness of the thin region is included in the formulation process. In the 2D and 3D geometries a triangular mesh and tetrahedral mesh will be considered, respectively.

4.1. The 2D Shell Element: A Rectangular Deformed Element

The line element shown in Figure 2(a) is the basis of the degenerated rectangular element. It is contructed by doubling the nodes of this line. The horizontal lines, created by this doubling, are defined by the nodes 1^-, 2^- and 1^+, 2^+ respectively (Fig. 2(b)). The nodal Whitney functions are defined by the next relations:

$$\begin{aligned}w^0_{i^-} &= w^0_{l_i}\alpha^- \\ w^0_{i^+} &= w^0_{l_i}\alpha^+\end{aligned} \tag{8}$$

where $w^0_{l_i}$ are the shape functions in a line element,

$$\begin{aligned}w^0_{l_1} &= 1/2(1-\xi) \\ w^0_{l_2} &= 1/2(1+\xi)\end{aligned} \tag{9}$$

These shape functions are projected on the lines Γ^- and Γ^+ by the coefficients α^- and α^+, noted as the doubling coefficients:

$$\begin{aligned}\alpha^- &= 1/2 - \eta/d \\ \alpha^+ &= 1/2 + \eta/d\end{aligned} \tag{10}$$

The nodal shape functions of a rectangular element will be thus formed by the nodal interpolation function in a 1D line element that are projected in the 2D space by the doubling coefficients. In a similar process, the edge

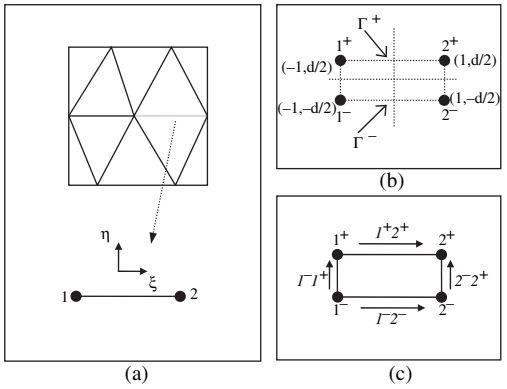

Fig. 2. 2D Rectangular shell element. (a) Element detail in a 2D mesh. (b) Nodal doubling. (c) Edge doubling.

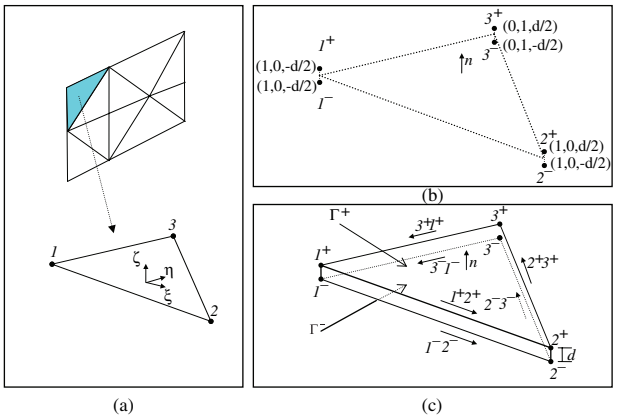

Fig. 3. The 3D shell element. (a) Element detail in a surface mesh. (b) Nodal doubling. (c) Edge doubling.

interpolation functions on the segments Γ^+ and Γ^- will be defined as a product between the edge interpolation functions in a line element and the doubling coefficients α^+ and α^- (Fig. 2(c)). The edge $1^- \rightarrow 2^-$ was named k^-. In the same way, the edge $1^+ \rightarrow 2^+$ on the line Γ^-, it is named k^+:

$$\begin{aligned} \boldsymbol{w}^1_{1^-2^-} &= \boldsymbol{w}^1_{k^-} = \boldsymbol{w}^1_{l_k}\alpha^- \\ \boldsymbol{w}^1_{1^+2^+} &= \boldsymbol{w}^1_{k^+} = \boldsymbol{w}^1_{\boldsymbol{l_k}}\alpha^+ \end{aligned} \tag{11}$$

where,

$$\boldsymbol{w}^1_{l_k} = (w^0_{l_1}\boldsymbol{grad}\, w^0_{l_2} - w^0_{l_2}\,\boldsymbol{grad}\, w^0_{l_1}) \tag{12}$$

is the classical definition of Whitney edge functions.

The edge interpolation functions of the perpendicular edges, $1^- \rightarrow 1^+$ and $2^- \rightarrow 2^+$, will be named thereafter as $1^\pm$ and $2^\pm$. They will be built following the same process established for the other edges:

$$\begin{aligned} \boldsymbol{w}^1_{1^\pm} &= (\alpha^-\,\boldsymbol{grad}\,\alpha^+ - \alpha^+\,\boldsymbol{grad}\,\alpha^-)w^0_{l_1} \\ \boldsymbol{w}^1_{2^\pm} &= (\alpha^-\,\boldsymbol{grad}\,\alpha^+ - \alpha^+\,\boldsymbol{grad}\,\alpha^-)w^0_{l_2} \end{aligned} \tag{13}$$

4.2. The 3D Shell Element: A Prism Deformed Element

In the 3D case, the shell element will be a deformation of a prismatic element.[5] The thin region represented by a surface mesh is shown in Figure 3(a). The deformed elements are constructed by doubling this surface mesh. The nodal interpolation functions are defined by (Fig. 3(b)):

$$\begin{aligned} w^0_{i^-} &= w^0_{t_i}\alpha^- \\ w^0_{i^+} &= w^0_{t_i}\alpha^+ \end{aligned} \tag{14}$$

where, w^0_{ti} are the nodal interpolation functions in a triangular element (Fig. 3(a)):

$$\begin{aligned} w^0_{t1} &= 1-\xi-\eta \\ w^0_{t2} &= \xi \\ w^0_{t2} &= \eta \end{aligned} \tag{15}$$

and the doubling coefficients are defined by:

$$\alpha^- = 1/2 - \zeta/d \quad \text{and} \quad \alpha^+ = 1/2 + \zeta/d \tag{16}$$

Using the same deduction process, the edge interpolation functions are defined by:

$$\begin{aligned} \boldsymbol{w}^1_{i^-j^-} &= \boldsymbol{w}^1_{k^-} = \boldsymbol{w}^1_{t_k}\alpha^- \\ \boldsymbol{w}^1_{i^+j^+} &= \boldsymbol{w}^1_{k^+} = \boldsymbol{w}^1_{t_k}\alpha^+ \end{aligned} \tag{17}$$

where, $\boldsymbol{w}^1_{t_k}$ are the edge interpolation functions in a triangular element that are defined by Eq. (12), using the appropriate nodal interpolation functions (Fig. 3(c)). The edge shape functions that connect the top and the bottom surfaces, Γ^+ and Γ^-, are defined by:

$$\boldsymbol{w}^1_{i^\pm} = \alpha^-\,\boldsymbol{grad}\,\alpha^+ - \alpha^+\boldsymbol{grad}\,\alpha^-)w^0_{t_i} \tag{18}$$

5. MAGNETODYNAMIC FORMULATIONS IN THIN REGIONS: SHELL ELEMENT APPROACH

The EC sensor considered in the problem description (Section 2) is a single coil placed above a thin conductive and/or ferromagnetic region. The first step for modeling this problem is to represent the thin region by a D-1 dimension object. In a 3D formulation, the thin region will be represented by its median surface and in a 2D formulation by its median line. In this way, during the mesh process (tetrahedral or triangular meshing), the thin region are skiped from this process. In the next step, during the construction of the discrete formulation problem, the volume integrals over the elements that represent the thin region (shell elements) are transformed by a surface integral. Finally, in the post-processing stage, the volume information is used again.

RESEARCH ARTICLE

5.1. 2D Shell Elements in the Electric Formulation a^*

Considering the axisymmetry of the problem geometry (Section 2), the most useful formulation is the electric one. In 2D, the modified magnetic vector potential $\boldsymbol{a}^*$ will have only an orthoradial vector component in a cylindrical coordinate system ($\boldsymbol{a}^*_\theta$). In consequence, the 2D problem will be reduced to calculate this scalar quantity. In the shell region, a^*_θ is discretised in each shell element by the nodal interpolation function

$$a^*_\theta = \sum_{i\in N} w^0_i a^*_{\theta_i} \tag{19}$$

where, the $a^*_{\theta_i}$ represent the nodal values of the modified vector potential a^*_θ in the mesh of the thin region. N is the set of nodes on the top and bottom line segments Γ^+ and Γ^-, such as $N \equiv N^+ \cup N^-$. In this way, the gradient of a^*_θ will be expressed as

$$\begin{aligned} \boldsymbol{grad}\, a^*_\theta &= \sum_{i\in N} \boldsymbol{grad}\,(w^0_i a^*_{\theta_i}) \\ &= \sum_{i^-\in N^-} \boldsymbol{grad}\,(w^0_{i^-} a^*_{\theta_{i^-}}) \\ &\quad + \sum_{i^+\in N^+} \boldsymbol{grad}\,(w^0_{i^+} a^*_{\theta_{i^+}}) \end{aligned} \tag{20}$$

and, the next equation result after some operations

$$\begin{aligned} \boldsymbol{grad}\, a^*_{\theta_i} = \sum_{i\in N}\Bigg(&\left[\alpha^- \boldsymbol{grad}\, w^0_{li} - \frac{w^0_{li}}{d}\boldsymbol{n}\right] a^*_{\theta_{i^-}} \\ &+ \left[\alpha^+ \boldsymbol{grad}\, w^0_{li}\frac{w^0_{li}}{d}\boldsymbol{n}\right] a^*_{\theta_{i^+}}\Bigg) \end{aligned} \tag{21}$$

where, $\boldsymbol{n}$ is an elementary vector in the perpendicular direction to the median line of the thin region. The weak formulation will be written using a cylindrical coordinate system. The first and fourth term of the Eq. (3) written in a vectorial form inside the thin region are defined by:

$$\begin{aligned} &\int_{\Omega_c} \frac{1}{\mu r}\left(\int_{-d/2}^{d/2} \boldsymbol{grad}\, r a^*_\theta \cdot (\boldsymbol{grad}\, r a'_\theta)^T\, dz\right) dr \\ &\int_{\Omega_c} \frac{i\omega\sigma}{r}\left(\int_{-d/2}^{d/2} r a^*_\theta (r a'_\theta)\, dz\right) dr \end{aligned} \tag{22}$$

where r is the radial distance in the cylindrical coordinate system.

5.2. 3D Shell Elements in the Magnetic Formulation $t-\phi$

The magnetic formulation with $\boldsymbol{t}-\phi$ potentials is the most currently used in 3D eddy current analysis because of its reduced number of degrees of freedom in comparison with the electric formulation, that use the combined $\boldsymbol{a}-\psi$ potentials.[9] In this case, only the scalar magnetic potential ϕ is calculated outside the conductive regions. In the regions that have a conductivity, it is necessary to compute the circulation over the edges of the electric vector potential $\boldsymbol{t}$, that are represented in the shell elements as:

$$\boldsymbol{t} = \sum_{k\in A} \boldsymbol{w}^1_k t_k + \sum_{i^\pm\in A_p} \boldsymbol{w}^1_{i^\pm} t_{n_{i^\pm}} \tag{23}$$

where A is the edge set over the surfaces Γ^+ and Γ^-, such that $A \equiv A^+ \cup A^-$; t_k is the field circulation along these edges and $t_{n_{i^\pm}}$ is the field circulation along the perpendicular edges A_p. Now, it is possible to calculate, using these approximations, the curl of the electric vector potential

$$\begin{aligned} \boldsymbol{curl}\, \boldsymbol{t} = &\sum_{k^-\in A^-}\left(\alpha^-\, \boldsymbol{curl}\, \boldsymbol{w}^1_{t_k} - \frac{1}{d}\boldsymbol{n}\times\boldsymbol{w}^1_{t_k}\right) t_{k^-} \\ &+\cdots \sum_{k^+\in A^+}\left(\alpha^+\, \boldsymbol{curl}\, \boldsymbol{w}^1_{t_k} + \frac{1}{d}\boldsymbol{n}\times\boldsymbol{w}^1_{t_k}\right) t_{k^+} \\ &+\cdots \sum_{i^\pm\in A_p}\left(\frac{1}{d}\boldsymbol{grad}\, w^0_{t_i}\times\boldsymbol{n}\right) t_{n_{i^\pm}} \end{aligned} \tag{24}$$

In this way, the first and third terms of the weak formulation can be written, in a vectorial form, inside the thin region as:

$$\begin{aligned} &\int_{\Omega_c} \frac{1}{\sigma}\left(\int_{-d/2}^{d/2} \boldsymbol{curl}\, \boldsymbol{t}\cdot(\boldsymbol{curl}\, \boldsymbol{t}')^T\, dz\right) d\Omega_S \\ &\int_{\Omega_c} i\omega\mu\left(\int_{-d/2}^{d/2} \boldsymbol{t}\cdot(\boldsymbol{t}')^T\, dz\right) d\Omega_S \end{aligned} \tag{25}$$

6. RESULTS

The parameters of the problem are synthetized in Table I. Two cases are considered in the modeling of the thin sheet. In the first case, the material has a low relative permeability and a high conductivity. In the second, it has a high relative permeability and a low conductivity. The resistance and reactance of the coil are calculated in function of the sheet thickness for both examples. It is observed (Figs. 4 and 5) that the electric formulation over-estimate the resistance, and under-estimate the reactance, the inverse situation is observed for the magnetic formulation.

In the high conductivity case (Fig. 4), the current induced in the shell has an important role. The $\boldsymbol{a}^*$ formulation inside the shell elements approximates the electrical field $\boldsymbol{e}$ as a linear function across the thickness since the shape functions are linear: the current density $\boldsymbol{j}$ will be linear. This is an acceptable approach to physical reality, especially, if the skin depth is relatively large compared with the shell thickness. As a consequence, the error over the resistance is less important. In $\boldsymbol{t}-\phi$ formulation the current density $\boldsymbol{j}$ is constant inside the shell elements since it is calculated by the curl operator ($\boldsymbol{curl}\, \boldsymbol{t} = \boldsymbol{j}$). This approximation is less adapted to physical reality; the error on the resistance is more important. The influence of the

Table I. Parameters and dimensions.

Coil parameters	
Inner radius	6.15 mm
Outer radius	12.3 mm
Height	6.15 mm
Number of turns	3790
Shell parameters	
High conductivity case	
Conductivity	30×10^6 S/m
Relative permeabiltity	1
High permeability case	
Conductivity	1×10^3 S/m
Relative permeabiltity	1×10^4
Other parameters	
Lift-off	0.88 mm
Frequency	900 Hz

magnetic field created by the induced currents is accuretly approximated in the $\boldsymbol{a}^*$ formulation since the magnetic energy, represented by the reactance, has a best approximation in the $\boldsymbol{a}^*$ formulation than in the $\boldsymbol{t}-\phi$.

In the high relative permeability case (Fig. 5), the magnetic field inside the shell has a more important role than the induced currents (low conductivity). In the $\boldsymbol{a}^*$ formulation, the linearity of the electrical field $\boldsymbol{e}$ across the thickness induces that the magnetic field $\boldsymbol{h}$, calculated by the curl operator, is constant: the error is more important on the reactance. In $\boldsymbol{t}-\phi$ formulation, the behaviour of shell elements is symmetrical: the magnetic field $\boldsymbol{h}$ has a linear variation across the thickness, the variation is more realistic, and the error on the reactance is less important. The agreement between these two formulations can be improved, in comparison with the analytical results, if the average values between the electric and magnetic formulations are considered (Figs. 4 and 5).

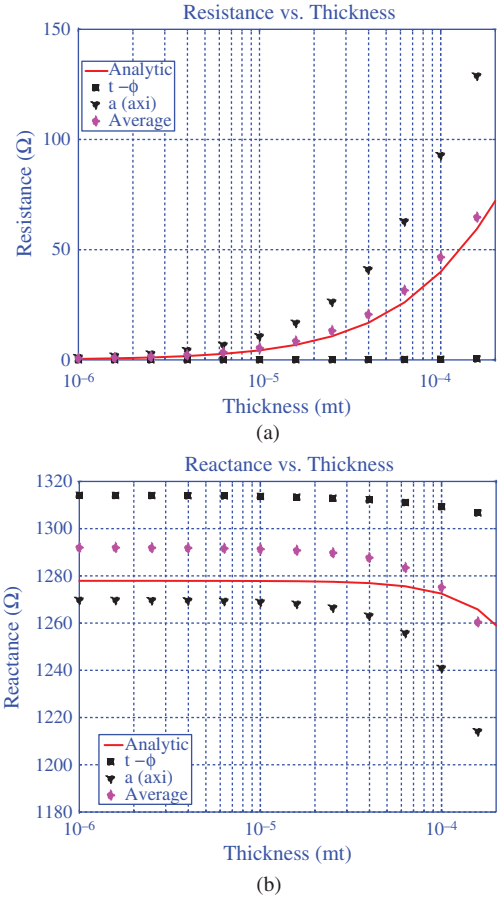

Fig. 4. High conductivity case. (a) Resistance variation. (b) Reactance variation.

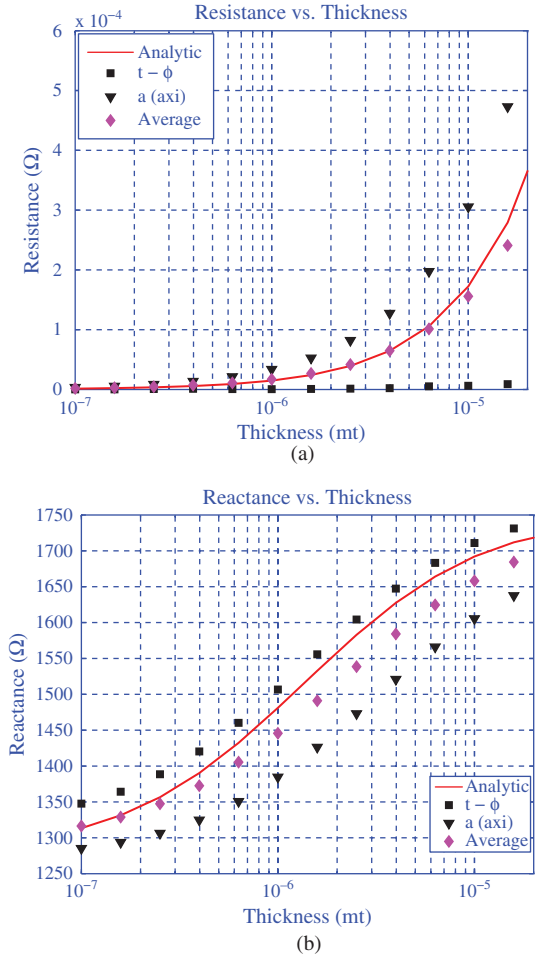

Fig. 5. High permeability case. (a) Resistance variation. (b) Reactance variation.

7. CONCLUSIONS

The shell elements represent an interesting solution for the calculation of the fields inside low thickness zones. They are obtained by deforming rectangular elements (2D) or prismatic elements (3D). In this way, they allow to reduce the dimensionality of the low thickness object. Consequently, they reduce and simplify the meshing process and the inversion of algebraic equations. The application of this kind of elements in FEM analysis, in

RESEARCH ARTICLE

the context of non-destructive testing by EC, is easy to implement. These elements fairly represent the physical phenomena inside the zones of low thickness when volumic meshing becomes complicated to realize (and even impossible in some cases).

References and Notes

1. J. R. Bowler, Y. Yoshida, and N. Harfield, *IEEE Transactions on Magnetics* 33, 4287 (**1997**).
2. J. Pavo, *IEEE Transactions on Magnetics* 40, 659 (**2004**).
3. C. Geuzaine, P. Dular, and W. Legros, *IEEE Transactions on Magnetics* 36, 799 (**2000**).
4. Y. Choua, L. Santandrea, Y. Le Bihan, and C. Marchand, *IEEE Transactions on Magnetics* 43, 1789 (**2007**).
5. Z. Ren, *IEEE Transactions on Magnetics* 34, 2547 (**1998**).
6. J. Gyselinck, R. V. Sabariego, and P. Dular, *COMPUMAG* (**2007**).
7. A. Bossavit, *IEEE Transactions on Magnetics* 32, 729 (**1996**).
8. P. Dular and C. Geuzaine, *IEEE Transactions on Magnetics* 39, 1139 (**2003**).
9. Z. Ren and A. Razek, *IEEE Transactions on Magnetics* 36, 751 (**2000**).
10. S. K. Burke, *J. Nondestruct. Eval.* 7, 35 (**1988**).